Acta Crystallographica Section F
Structural Biology and Crystallization Communications
ISSN 1744-3091

The taming of small heat-shock proteins: crystallization of the α-crystallin domain from human Hsp27

E. V. Baranova,[a]* S. Beelen,[a] N. B. Gusev[b] and S. V. Strelkov[a]*

[a]Laboratory for Biocrystallography, Department of Pharmaceutical Sciences, Katholieke Universiteit Leuven, Belgium, and [b]Department of Biochemistry, School of Biology, Moscow State University, Russia

Correspondence e-mail: ebaranov@vub.ac.be, sergei.strelkov@pharm.kuleuven.be

Received 31 August 2009
Accepted 26 October 2009

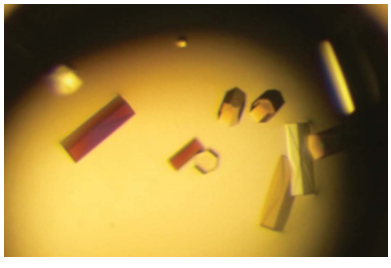

Small heat-shock proteins (sHsps) are ubiquitous molecular chaperones. sHsps function as homooligomers or heterooligomers that are prone to subunit exchange and structural plasticity. Here, a procedure for obtaining diffraction-quality crystals of the α-crystallin domain of human Hsp27 is presented. Initially, limited proteolysis was used to delineate the corresponding stable fragment (residues 90–171). This fragment could be crystallized, but examination of the crystals using X-rays indicated partial disorder. The surface-entropy reduction approach was applied to ameliorate the crystal quality. Consequently, a double mutant E125A/E126A of the 90–171 fragment yielded well ordered crystals that diffracted to 2.0 Å resolution.

1. Introduction

Small heat-shock proteins (sHsps) form a large and heterogeneous family of ubiquitous proteins that are expressed in bacteria, fungi, plants and animals (Nakamoto & Vigh, 2007). By interacting with denatured proteins and preventing their aggregation, sHsps serve as promiscuous molecular chaperones that protect the cell against unfavourable conditions such as heat shock, ischaemia or oxidative stress.

Although sHsps vary in sequence and in size, they have a common overall structure which most importantly includes a distinct conserved β-sandwich domain named the α-crystallin domain that comprises about 90 residues (Kim *et al.*, 1998; van Montfort *et al.*, 2001). This domain is preceded by a highly variable N-terminal region and is followed in most cases by a short and flexible C-terminal extension. sHsp monomers range in size from 12 to 43 kDa (Haslbeck *et al.*, 2005; Nakamoto & Vigh, 2007). Importantly, in mammalian cells functional sHsps are almost always found as homooligomeric or heterooligomeric complexes with molecular masses of between 50 and about 800 kDa (Arrigo *et al.*, 2007). This oligomeric structure is highly dynamic.

Accumulation of aggregates of denatured proteins is characteristic of many human diseases such as desmin-related myopathy, cataracts and neurodegenerative diseases (Clark & Muchowski, 2000; Haslbeck *et al.*, 2005). By preventing the aggregation of unfolded proteins, sHsps can slow or even prevent the development of these diseases. At the same time, the number of detected sHsp point mutations is increasing rapidly; these mutations are believed to compromise their function in diseased tissue (Evgrafov *et al.*, 2004; Irobi *et al.*, 2004).

To date, only three crystal structures of full-length sHsps have been determined: those of *Methanococcus jannaschii* Hsp16.5 (Kim *et al.*, 1998), wheat Hsp16.9 (van Montfort *et al.*, 2001) and Tsp36 from the parasitic flatworm *Taenia saginata* (Stamler *et al.*, 2005). The main reason for the lack of high-resolution X-ray data on full-length mammalian sHsps is the difficulty in obtaining diffraction-quality three-dimensional crystals. This difficulty is apparently linked to the intrinsic polydispersity of the full-length protein, since obtaining a conformationally homogeneous protein population is generally known to be a prerequisite for crystal growth.

In this study, we used limited proteolysis to delineate the stable domains of human Hsp27 and Hsp22, which are heat-inducible members of the sHsp family (Arrigo *et al.*, 2007; Shemetov *et al.*, 2008). As a result, we were able to crystallize the α-crystallin domain

of human Hsp27. Rational design of mutations *via* the surface-entropy reduction approach was indispensable in obtaining well diffracting crystals.

2. Materials and methods

2.1. Limited proteolysis

Recombinant full-length Hsp27 was purified as described previously (Bukach *et al.*, 2004) and digested by trypsin for 1 h at 293 K at a Hsp27:trypsin mass ratio of 1000:1 in 50 m*M* Tris–HCl pH 8.0 containing 5 m*M* NaCl, 0.5 m*M* $CaCl_2$ and 7 m*M* β-mercaptoethanol. At selected time points, 10 µl aliquots were removed and the reaction was quenched by the addition of 1 µl 100 m*M* phenylmethanesulfonyl fluoride (PMSF). The samples were analyzed by SDS–PAGE on 16.5% gels according to Schägger & von Jagow (1987). The protein bands were stained with Coomassie R250. N-terminal sequencing was performed using an Applied Biosystems 491 sequencer after transfer of the peptides onto polyvinylidene difluoride membrane. C-terminal sequencing was performed using a carboxypeptidase (A and B) mixture and an automatic Biotronik LC 3000 amino-acid analyzer.

2.2. Cloning and purification of fragments

All sHsp fragments were cloned, expressed and purified using the pPEP-TEV vector essentially as described previously (Strelkov *et al.*, 2004). Briefly, each fragment was expressed in *Escherichia coli* strain BL21 (DE3) as a fusion product starting with an N-terminal 6×His tag followed by a 7 kDa spacer domain, a tobacco etch virus (TEV) protease-cleavage site and the sHsp fragment. Purification was achieved by affinity chromatography on a nickel-chelating column under native conditions followed by removal of the His tag and spacer using TEV protease also containing a His tag. Size-exclusion chromatography was performed on a Superdex 75 HiLoad 16/60 column calibrated with ovalbumin (43 kDa), chymotrypsinogen (25 kDa) and ribonuclease A (13.7 kDa) as molecular-weight markers. The QuikChange site-directed mutagenesis kit (Stratagene, La Jolla, California, USA) was used to prepare the mutated protein variants and the presence of mutations was verified by DNA sequencing.

2.3. Crystallization and data collection

Purified proteins were concentrated to 8 mg ml^{-1} in 10 m*M* Tris–HCl pH 8.0, 25 m*M* NaCl, 1 m*M* DTT, 1 m*M* EDTA and 1 m*M* NaN_3. In the case of the 90–171 E125A/E126A fragment, the non-detergent sulfobetaine 195 (NDSB-195) was included in the protein solution at a final concentration of 200 m*M*. Extensive screening of crystallization conditions from commercially available kits was performed manually using the hanging-drop vapour-diffusion method. For each sample, 300–500 different precipitation solutions were tested at both 277 and 293 K. The best crystals were obtained at 277 K by mixing equal volumes (1 µl) of protein and precipitant solution and equilibrating against 500 µl precipitant solution.

The optimized crystals were briefly transferred into a cryoprotectant solution containing the precipitant solution supplemented with 30%(*v*/*v*) glycerol and flash-cooled in liquid nitrogen. X-ray diffraction data were collected at the SLS synchrotron (Villigen, Switzerland) using MAR CCD and Pilatus detectors at 100 K. Diffraction images were analyzed using *HKL*-2000 (Otwinowski & Minor, 1997). Data were processed using *XDS* (Kabsch, 1993) and *SCALA* (Evans, 2006) (Table 1).

Table 1
Data-collection statistics.

Values in parentheses are for the highest resolution shell.

	First crystal form	Second crystal form
Space group	*P*622	*P*622
Unit-cell parameters (Å)	$a = b = 76.4$, $c = 65.1$	$a = b = 74.5$, $c = 120.0$
Molecules per ASU	1	2
V_M (Å^3 Da^{-1})	2.95	2.61
Data collection		
Wavelength (Å)	0.9878	0.9999
Resolution range (Å)	46.4–2.0 (2.11–2.0)	43.9–2.2 (2.3–2.2)
Unique reflections	8007 (1123)	10572 (1495)
Completeness (%)	100 (100)	100 (100)
Average $I/\sigma(I)$	23.9 (4.7)	15.7 (4.0)
R_{merge}† (%)	4.8 (47.0)	7.2 (76.0)
R_{meas}† (%)	5.1 (49.7)	7.6 (80.0)
Multiplicity	9.3 (9.5)	9.4 (9.5)

† $R_{merge} = \sum_{hkl}\sum_i |I_i(hkl) - \langle I(hkl)\rangle| / \sum_{hkl}\sum_i I_i(hkl)$, $R_{meas} = \sum_{hkl}[N/(N-1)]^{1/2} \sum_i |I_i(hkl) - \langle I(hkl)\rangle| / \sum_{hkl}\sum_i I_i(hkl)$, where $I_i(hkl)$ is the ith observation of $I(hkl)$, $\langle I(hkl)\rangle$ is the mean of N measurements (Diederichs & Karplus, 1997).

3. Results and discussion

3.1. Stable domains of human sHsp27 identified by limited proteolysis

In our hands, extensive crystallization trials using full-length human Hsp27, Hsp22 and the K141E mutant of Hsp22, the expression of which correlates with motor neuropathy (Irobi *et al.*, 2004),

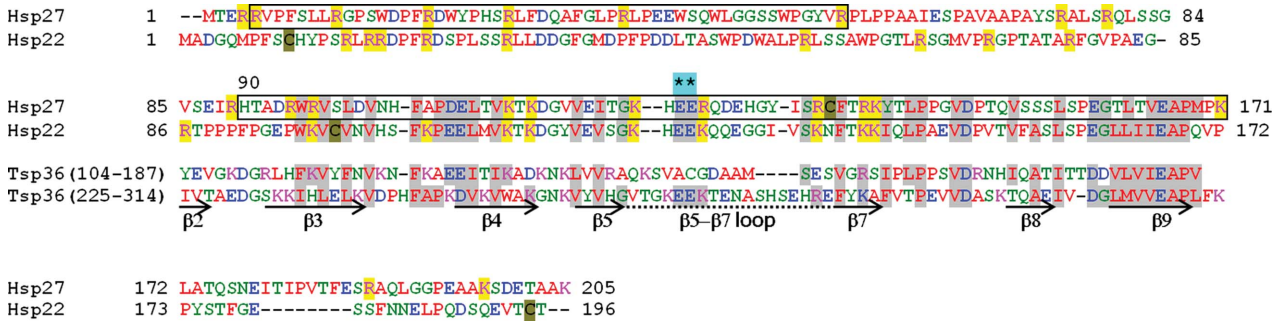

Figure 1
Sequence alignment of human Hsp27, human Hsp22 and two *T. saginata* Tsp36 α-crystallin domains (ACD1 and ACD2). The alignment was produced using *ClustalW* (Thompson *et al.*, 1994) with minor manual editing. The conserved regions are shaded in grey. Potential trypsin-cleavage sites after Arg and Lys residues in the Hsp22 and Hsp27 sequences are highlighted in yellow, negatively charged residues are marked in blue and Cys residues are shaded in mossy green. Purified proteolytic fragments of Hsp27 are boxed. The secondary-structure elements shown are as in the Tsp36 crystal structure. Residues Glu125 and Glu126 of the Hsp27 sequence that were chosen for mutagenesis are marked with asterisks.

were not successful. To circumvent this difficulty, we decided to determine the stable domains within these sHsps using limited proteolysis. In particular, specific trypsin digestion is potentially possible after any Arg or Lys residue, both of which are abundant along the whole length of both sHsps (Fig. 1), providing a prerequisite for obtaining a proteolytic fragment that would correspond to a distinct protein domain. In agreement with previous work (Kim *et al.*, 2006), we found that human Hsp22 and its K141E mutant were very susceptible to trypsinolysis and rapidly hydrolyzed to very short fragments (data not shown). Limited trypsinolysis of Hsp27 led to the formation of two distinct fragments with apparent molecular masses of about 6.5 and 9 kDa, respectively (Fig. 2). N-terminal and C-terminal sequencing of the 6.5 kDa fragment revealed that it includes residues 5–56 of Hsp27. N-terminal sequencing of the 9 kDa fragment indicated His90 to be the starting residue. This fragment was estimated to extend to Lys171 judging by its molecular mass and the available cleavage sites. Sequence alignment with the known crystal structures of sHsps (Fig. 1) suggests that the 90–171 fragment of Hsp27 corresponds to the α-crystallin domain without the flexible N-terminal and C-terminal extensions.

3.2. Purification and properties of the Hsp27 90–171 fragment

The resulting fragment 5–56 was insoluble, whereas the fragment 90–171 was obtained in a soluble state in milligram quantities. As a final purification stage, this fragment was subjected to size-exclusion chromatography on a Superdex 75 HiLoad 16/60 column in 50 m*M* Tris–HCl pH 8.0 buffer containing 150 m*M* NaCl and 1 m*M* DTT. Under these conditions, the fragment eluted as a sharp peak with an apparent molecular mass of 25 kDa. This suggested that this fragment forms dimers or trimers under the conditions used. More recently, we have carried out dynamic light-scattering and small-angle X-ray scattering measurements on Hsp27 90–171 solutions. These experiments (manuscript in preparation) consistently indicated that the fragment exists as a dimer in solution.

3.3. Partially disordered crystals of the 90–171 fragment

Crystallization screening with several hundred precipitant solutions yielded crystals in a single condition from the JCSG crystallization screen. After optimization, plate-like crystals (0.2 × 0.08 × 0.05 mm) appeared after approximately 1 d with a reservoir solution containing 2.2 *M* ammonium sulfate, 0.2 *M* ammonium chloride pH 5.5 (Fig. 3*a*). X-ray analysis of the obtained crystals revealed diffraction to 2.5 Å resolution. However, these crystals appeared to be partially disordered in one direction. When the incident beam was roughly perpendicular to the plane of the plate-like crystals, the diffraction pattern revealed sharp reflections. When the crystal was rotated by 90°, long streaks were observed in one direction, as seen in Fig. 3(*c*). This tendency persisted in both flash-cooled and room-temperature crystals. Moreover, screening various additives during crystallization did not improve the quality of crystals.

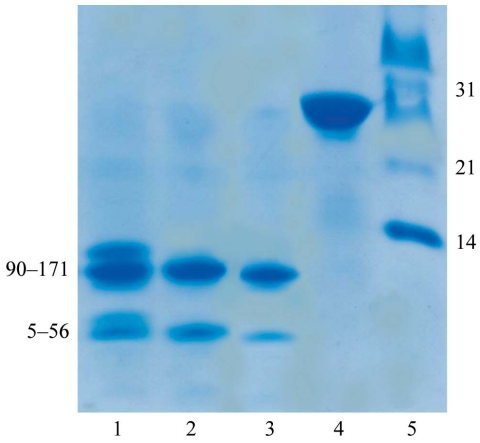

Figure 2
Kinetics of Hsp27 trypsinolysis analyzed by SDS–PAGE. Lanes 1–3, Hsp27 after 30, 40 and 60 min digestion, respectively. Lane 4, original Hsp27 sample. Lane 5, molecular-weight markers (labelled in kDa).

In a further attempt to overcome these crystallization difficulties, we purified 90–171 fragments containing the disease-related Hsp27 mutations S135F, R136W and R127W. These mutations correlate with Charcot–Marie–Tooth disease (S135F, R136W) and distal hereditary motor neuropathy (R127W, S135F) (Evgrafov *et al.*, 2004). Attempts to crystallize the R136W and R127W mutants were unsuccessful, whereas the S135F mutant crystallized; however, these crystals had an intrinsic disorder like those of the wild-type fragment.

3.4. Improving the crystal quality using rational mutagenesis

We considered that the observed disorder within the Hsp27 90–171 fragment crystals might arise from surface-exposed regions of the polypeptide chain that were suboptimal for the formation of stable crystal lattice contacts. To ameliorate this problem, a rational mutagenesis approach ('surface engineering') has been proposed (Goldschmidt *et al.*, 2007). By using the *SERp* (*Surface Entropy Reduction prediction*) web server at http://www.doe-mbi.ucla.edu/Services/SER with default parameters, we detected the leading cluster with the highest calculated entropy within the 90–171 fragment. This cluster included residues 125–130 (EERQDE; *SERp* score 3.52). These residues are located in the middle of the α-crystallin domain in the loop connecting the fifth and seventh β-strands (Fig. 1). To reduce the surface entropy, a concurrent mutation of residues Glu125 and Glu126 was proposed. The evolutionary conservation of these residues within the family of small heat-shock proteins is quite high: both residues are present in the sequences of human Hsp22, Hsp20, αB-crystallin and the second α-crystallin domain of Tsp36 (Fig. 1).

The replacement of the selected residues by an alanine or their deletion (Δ) were chosen to give two alternative approaches. To enhance the probability of crystallization, we cloned and expressed three different multiple mutants of the Hsp27 90–171 fragment: E125A/E126A, E125Δ/E126Δ/Q128A/E130A and E125Δ/E126Δ/Q128Δ/E130Δ. The purification of the two mutants containing deletions was complicated by problems in cleaving the fusion expression product using TEV protease, which might arise from inappropriate folding of the fusions.

3.5. Properties, crystallization and preliminary X-ray data of the 90–171 E125A/E126A fragment

Size-exclusion chromatography with the 90–171 E125A/E126A fragment yielded elution profiles that were indistinguishable from those of the wild-type (WT) 90–171 fragment. Therefore, we conclude that the introduced mutations do not significantly affect its oligomeric state. The E125A/E126A fragment crystals could be grown from protein solutions containing 200 m*M* NDSB-195 after 1 d using a reservoir solution consisting of 2.2 *M* ammonium sulfate, 0.2 *M* diammonium tartrate pH 5.5, *i.e.* under conditions closely resembling those used for the WT fragment. The appearance of these crystals as tall hexagonal prisms (Fig. 3*b*) was distinct from those of the WT fragment (Fig. 3*a*).

Importantly, the diffraction pattern for the Hsp27 90–171 E125A/E126A variant (Fig. 3*d*) revealed an ordered lattice in all directions

and could be readily processed. The crystals belonged to space group *P*622, with unit-cell parameters $a = b = 76.4$, $c = 65.1$ Å. The asymmetric unit contained one monomer, with a V_M value of 2.95 Å^3 Da^{-1} (Matthews, 1968) and a solvent content of 59%. A full diffraction data set could be collected to 2.0 Å resolution using a synchrotron X-ray source (Table 1). Attempts to phase these data using molecular replacement with known α-crystallin domain structures are under way. In addition, a second well ordered crystal form of the Hsp27 90–171 E125A/E126A fragment could be obtained. This form belonged to the same space group *P*622, with unit-cell parameters $a = b = 74.5$, $c = 120$ Å and two monomers per asymmetric unit.

At this point, the partially disordered diffraction pattern of the WT fragment could be superimposed with a hexagonal lattice with $a = b = 76.0$, $c = 63.1$ Å, *i.e.* close to the unit-cell parameters of the mutant fragment (Fig. 3*e*). There is proper order along the a^* and b^* lattice directions. Furthermore, the (0, 0, *l*) reflections are clearly resolved but most other reflections are heavily smeared in the c^* direction (Fig. 3*e*). This led us to the hypothesis that the observed pattern could arise from a screw axis in the c^* direction [and hence systematic absences for the (0, 0, *l*) reflections], with the same *a* cell edge and a longer *c* edge. The three possibilities here are a lattice with a 6_3 screw axis and $c = 126.2$ Å, a lattice with a $6_2/6_4$ axis and $c = 189.3$ Å or a lattice with a $6_1/6_5$ axis and $c = 378.6$ Å. Since the X-ray data-collection setup used allows the resolution of spots for up to ∼500 Å cell edges, even assuming the longest possible *c*-edge value (378.6 Å) the observed smearing could not be explained simply by an overlap of reflections. We conclude that the crystal-packing arrangement of the WT fragment resembles that of the mutant but might involve a larger cell with several monomers per asymmetric unit and some differences in the symmetry. In any case, the observed

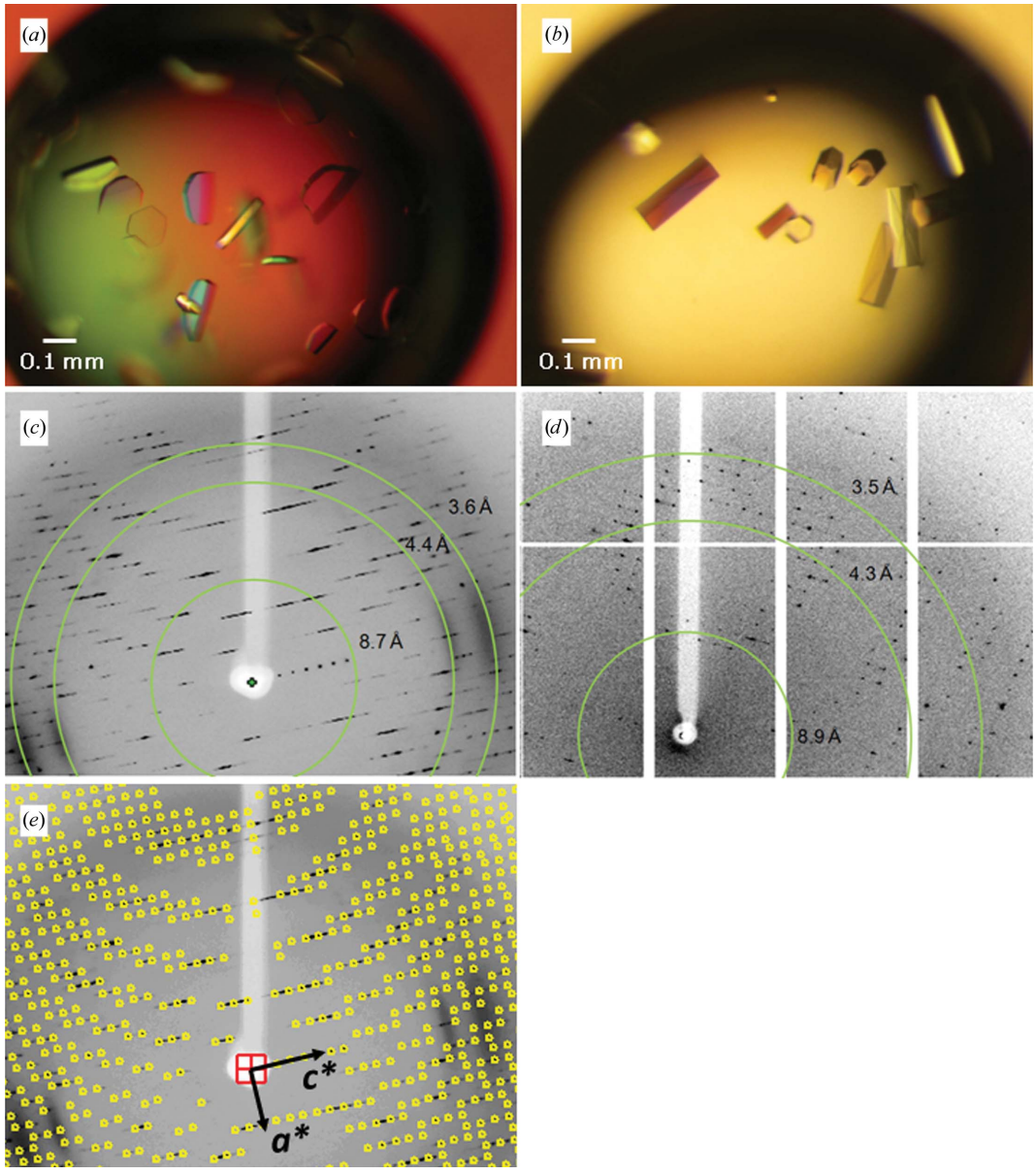

Figure 3
Crystallization and diffraction patterns of the wild-type and mutated Hsp27 90–171 fragments. (*a*) Crystals of the wild-type fragment (maximum dimensions 0.17 × 0.08 × 0.05 mm). (*b*) Crystals of the E125A/E126A fragment (maximum dimensions 0.3 × 0.1 × 0.1 mm). (*c*) X-ray diffraction pattern from the WT fragment crystals showing partial disorder. (*d*) Diffraction pattern from the E125A/E126A crystals indicating a well ordered crystal lattice. (*e*) Indexing of the diffraction pattern shown in (*c*) assuming a hexagonal lattice with $a = 76.0$, $c = 63.1$ Å.

smearing suggests that the stacking of molecules in the *c* direction is prone to some irregularity.

4. Concluding remarks

The α-crystallin domain of sHsps has been shown to be involved in the substrate-binding and chaperone activity as well as in formation of the dimer interface (Koteiche & McHaourab, 2002; Ghosh *et al.*, 2008). Determination of its crystal structure is clearly indispensable in order to understand these functional features. Very recently, crystal structures of the α-crystallin domain from rat Hsp20 and from human αB-crystallin have been reported (Bagneris *et al.*, 2009). In these cases the crystallizable domain was also derived using limited proteolysis.

The presented results for the α-crystallin domain from human sHsp27 point to several noteworthy features of the loop connecting the β5 and β7 strands in the middle of the α-crystallin domain. On one hand, this relatively long loop (with a predicted length of 13 residues) was not digested upon limited proteolysis by trypsin even though it contains two Arg residues. This suggests that this loop remains protected in wild-type Hsp27 and should be involved in intrasubunit and/or intersubunit contacts. On the other hand, the engineered double mutation E125A/E126A that ameliorated the crystal disorder is located at the beginning of this loop. This suggests that residues 125 and 126 are involved in contacts between monomers in the crystal lattice.

We thank Drs Lidiya Kurochkina, Mikhail Schneider and Natalya Khoroshilova (Institute of Bioorganic Chemistry, Moscow) for help with the limited proteolysis experiments and protein sequencing. EVB was funded by the OE Doctoral Fellowship from the Katholieke Universiteit Leuven. This research was supported by grants G.0697.08 from the Flanders Research Foundation (FWO) and OT 07/071 from the Katholieke Universiteit Leuven to SVS and the Russian Fund for Basic Research to NBG. The X-ray data collection was made possible by the Swiss Light Source synchrotron facility beamlines PX and PXIII.

References

Arrigo, A. P., Simon, S., Gibert, B., Kretz-Remy, C., Nivon, M., Czekalla, A., Guillet, D., Moulin, M., Diaz-Latoud, C. & Vicart, P. (2007). *FEBS Lett.* **581**, 3665–3674.
Bagneris, C., Bateman, O. A., Naylor, C. E., Cronin, N., Boelens, W. C., Keep, N. H. & Slingsby, C. (2009). *J. Mol. Biol.* **392**, 1242–1252.
Bukach, O. V., Seit-Nebi, A. S., Marston, S. B. & Gusev, N. B. (2004). *Eur. J. Biochem.* **271**, 291–302.
Clark, J. I. & Muchowski, P. J. (2000). *Curr. Opin. Struct. Biol.* **10**, 52–59.
Diederichs, K. & Karplus, P. A. (1997). *Nature Struct. Biol.* **4**, 269–275.
Evans, P. (2006). *Acta Cryst.* D**62**, 72–82.
Evgrafov, O. V. *et al.* (2004). *Nature Genet.* **36**, 602–606.
Ghosh, J. G., Houck, S. A. & Clark, J. I. (2008). *Int. J. Biochem. Cell Biol.* **40**, 954–967.
Goldschmidt, L., Cooper, D. R., Derewenda, Z. S. & Eisenberg, D. (2007). *Protein Sci.* **16**, 1569–1576.
Haslbeck, M., Franzmann, T., Weinfurtner, D. & Buchner, J. (2005). *Nature Struct. Mol. Biol.* **12**, 842–846.
Irobi, J. *et al.* (2004). *Nature Genet.* **36**, 597–601.
Kabsch, W. (1993). *J. Appl. Cryst.* **26**, 795–800.
Kim, K. K., Kim, R. & Kim, S.-H. (1998). *Nature (London)*, **394**, 595–599.
Kim, M. V., Kasakov, A. S., Seit-Nebi, A. S., Marston, S. B. & Gusev, N. B. (2006). *Arch. Biochem. Biophys.* **454**, 32–41.
Koteiche, H. A. & McHaourab, H. S. (2002). *FEBS Lett.* **519**, 16–22.
Matthews, B. W. (1968). *J. Mol. Biol.* **33**, 491–497.
Montfort, R. L. van, Basha, E., Friedrich, K. L., Slingsby, C. & Vierling, E. (2001). *Nature Struct. Biol.* **8**, 1025–1030.
Nakamoto, H. & Vigh, L. (2007). *Cell. Mol. Life Sci.* **64**, 294–306.
Otwinowski, Z. & Minor, W. (1997). *Methods Enzymol.* **276**, 307–326.
Schägger, H. & von Jagow, G. (1987). *Anal. Biochem.* **166**, 368–379.
Shemetov, A. A., Seit-Nebi, A. S. & Gusev, N. B. (2008). *J. Neurosci. Res.* **86**, 264–269.
Stamler, R., Kappé, G., Boelens, W. & Slingsby, C. (2005). *J. Mol. Biol.* **353**, 68–79.
Strelkov, S. V., Kreplak, L., Herrmann, H. & Aebi, U. (2004). *Methods Cell Biol.* **78**, 25–43.
Thompson, J. D., Higgins, D. G. & Gibson, T. J. (1994). *Nucleic Acids Res.* **22**, 4673–4680.